Natural Hazards
https://doi.org/10.1007/s11069-023-05841-1

ORIGINAL PAPER

Estuarine response to storm surge and sea-level rise associated with channel deepening: a flood vulnerability assessment of southwest Louisiana, USA

Maqsood Mansur[1] · Julia Hopkins[1,2] · Qin Chen[1,2]

Received: 14 July 2022 / Accepted: 26 January 2023

Abstract
This study investigates the sensitivity of the Calcasieu Lake estuarine region to channel deepening in southwest Louisiana in the USA. We test the hypothesis that the depth increase in a navigational channel in an estuarine region results in the amplification of the inland penetration of storm surge, thereby increasing the flood vulnerability of the region. We run numerical experiments using the Delft3D modeling suite (validated with observational data) with different historic channel depth scenarios. Model results show that channel deepening facilitates increased water movement into the lake–estuary system during a storm surge event. The inland peak water level increases by 37% in the presence of the deepest channel. Moreover, the peak volumetric flow rate increases by 291.6% along the navigational channel. Furthermore, the tidal prism and the volume of surge prism passing through the channel inlet increase by 487% and 153.3%, respectively. In our study, the presence of the deepest channel results in extra 56.72 km^2 of flooded area (approximately 12% increase) which is an indication that channel deepening over the years has rendered the region more vulnerable to hurricane-induced flooding. The study also analyzes the impact of channel deepening on storm surge in estuaries under different future sea-level rise (SLR) scenarios. Simulations suggest that even the most conservative scenario of SLR will cause an approximately 51% increase in flooded area in the presence of the deepest ship channel, thereby suggesting that rising sea level will cause increased surge penetration and increased flood risk.

Keywords Channel deepening · Storm surge · Estuarine region · Coastal flood vulnerability · Hurricane Laura · Sea-level rise

✉ Julia Hopkins
j.a.hopkins@northeastern.edu

[1] Civil and Environmental Engineering, Northeastern University, Boston, MA 02115, USA

[2] Marine and Environmental Sciences, Northeastern University, Boston, MA 02115, USA

1 Introduction

Global climate change is expected to intensify the strength of hurricanes (Emanuel 2005, 2020; Knutson et al. 2010; references therein and many others). Despite some debate, the frequency of hurricanes is anticipated to escalate as well (Holland and Webster 2007; Emanuel 2021; Vecchi et al. 2021; Klotzbach et al. 2022; references therein and many others). Moreover, rising sea levels are expected to exacerbate the flooding caused due to the storm surges associated with these tropical cyclones, posing a dire threat to life and property of coastal communities (Karim and Mimura 2008; Shepard et al. 2012; Tasnim et al. 2015; references therein and many others). Coincident with climate change are anthropogenic modifications to coastal areas—channelization and dredging for shipping purposes, reclamation, diking, filling of intertidal and shallow subtidal waters, hardening of shorelines and regulating river discharges. These anthropogenic developments have resulted in some adverse consequences, such as (1) increased salinity due to saltwater intrusion that threatens drinking water supplies (Kim and Johnson 1998; Ralston and Geyer 2019; Siles-Ajamil et al. 2019); (2) circulation and exchange flow alterations affecting salinity (Zhu et al. 2015; Chant et al. 2018; Wang and Shen 2020); (3) increased risk of erosion due to increase in the tidal prism (Cox et al. 2003); (4) tidal range, current and energy alterations that changes sediment transport patterns (Pareja-Roman et al. 2020); (5) increased sediment concentration (Kerner 2007; van Maren et al. 2015; Dijkstra et al. 2019) and upstream movement of estuarine turbidity maximum (de Jonge et al. 2014; Burchard et al. 2018) affecting ecology and water quality; (6) decrease in dissolved oxygen (Kaur et al. 2007; Sangita et al. 2014); (7) flow and discharge augmentation that causes sediment regime alteration (Rahman and Yunus 2016); and (8) storm surge and tidal amplification (Familkhalili and Talke 2016; Ralston et al. 2019; Familkhalili et al. 2020; Talke et al. 2021; references therein and many others).

Channel deepening can have varying effects on the water-level dynamics of a given location during any given storm event. Although it usually increases the water level resulting from storm surge and tidal amplification, it can lead to attenuated mean water level (Jensen et al. 2003; Jay et al. 2011; Ralston et al. 2019) and tidal amplitude (Cai et al. 2012a) as well, owing to increased hydraulic conveyance. There may even be no relationship between channel deepening and storm surge and tidal dynamics (Cai et al. 2012a; Bilskie 2013). Thus, the same process of channel deepening can both increase and decrease the total water level. The geometric properties of an estuary play a vital role in this regard since tidal dynamics and the friction to water movement depend on depth, cross-sectional area, width, convergence and other bathymetric properties (Friedrichs and Aubrey 1994; Orton et al. 2015; Familkhalili and Talke 2016).

Moreover, the impact of sea-level rise (SLR) on coastal flooding is uncertain on its own. The flood area does not always increase because of SLR, particularly in tidal river estuaries, where streamflows and the resulting hydraulic head in the upriver location control storm-driven flood levels (Orton et al. 2020) and where water levels are primarily influenced by the freshwater discharges (Chen and Liu 2016). Thus, climate change and its associated uncertainties suggest the importance of incorporating climate change effects in a coastal hazard risk assessment. In spite of increasing demand for the integration of climate change adaptation and disaster risk reduction, effective integration of the two in the disaster management planning process remains limited due to logistical problems associated with funding; lack of quality governance, coordination, collaboration, implementation, mainstreaming and community involvement; geopolitical factors; and

information, knowledge and policy gaps (Mitchell et al. 2010; Gero et al. 2011; Serrao-Neumann et al. 2015; Islam et al. 2020).

In this paper, we investigate the sensitivity of the Calcasieu Lake estuarine region in southwest Louisiana (Fig. 1) to the common anthropogenic modification of channel deepening. We study the changes in storm surge and flood vulnerability in the estuarine region that can be tied to water depth changes of the Calcasieu Ship Channel. This is critical in the sense that the Calcasieu Lake estuarine region is one of Louisiana's most at-risk hurricane zones and is prone to widespread flooding (Rego et al. 2010; Manning 2021). Regardless of the hurricane and flood risk, the region is one of America's most active energy corridors, with the country's 6th largest refinery, two of the country's largest liquefied natural gas (LNG) facilities, a complex of energy pipelines and the Henry Hub, a major natural gas hub for the USA. The port also serves as a big driver of the country's GDP, which is an estimated $39 billion (Calcasieu Ship Channel 2021; Martin Associates 2021). To sustain such heavy port activities, channel deepening is essential for navigation. However, the impact of channel deepening on ecological and environmental integrity is a major concern.

Despite all the previous studies on the various adverse consequences of channel deepening, little focus has been given on how the water level responds or storm surge propagates inland during a hurricane owing to the presence of a deepened channel in an estuarine region. Our study aims to fill this knowledge gap by testing the hypothesis that the deepening of the Calcasieu Ship Channel has increased the flood vulnerability of the Calcasieu Lake estuarine region. We accomplish this using the Delft3D modeling suite based on measured 1874, 1903, 1941 and 2020 channel bathymetric conditions, thereby testing our hypothesis on a broad, shell-shaped, sluggish lake–estuary system using measured meteorological forcing data of Hurricane Laura (2020). We also incorporate SLR effects in our study by analyzing the impact of channel deepening on storm surge in estuaries under future sea-level rise scenarios.

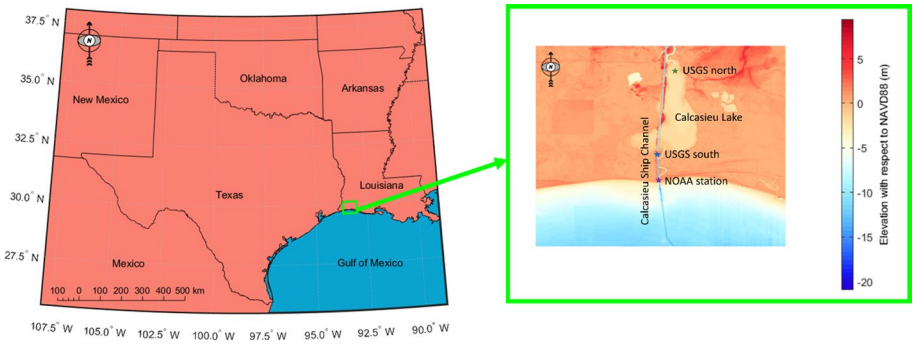

Fig. 1 Site map of the Calcasieu Lake estuarine region in southwest Louisiana. The light green rectangle marks the study domain in the estuarine region. The figure on the right shows the zoomed-in study domain and the locations of Calcasieu Lake, Calcasieu Ship Channel and the NOAA and USGS water-level stations. The color bar shows the elevation with respect to NAVD88 in meters

2 Methodology

2.1 Study domain

Calcasieu Lake is a large, shallow, brackish lake in southwestern Louisiana (Lee et al. 1990; Wang et al. 2020). The lake is surrounded by brackish marsh and runs approximately 28 km from north to south. The broad southern shore extends approximately 19 km in the east–west direction. Calcasieu Lake is connected to the Gulf of Mexico through a narrow, 9 km channel called the Calcasieu Pass. Apart from the channel, the estuarine region is shallow with an average depth of 2 m. The region is part of the Calcasieu-Sabine Basin.

Like many estuaries of the world, this lake–estuary system is no longer in its natural configuration owing to the Calcasieu Ship Channel, which is maintained at 40 feet (12.19 m) deep by 400 feet (121.92 m) wide and extends from the Gulf of Mexico to Lake Charles (CWPPRA 1992; McGinnis et al. 2019). The U.S. Army Corps of Engineers (USACE) first constructed the 5-feet-deep × 80-feet-wide × 7500-feet-long (1.52 m × 24.38 m × 2286 m) channel in 1874. Since 1874, the navigational channel has been dredged and widened several times leading to alterations in the hydrology and water quality of the estuarine region (McGinnis et al. 2019). In 1903, the channel was deepened to 13 feet (3.96 m) and was completed in 1941 with a depth of 30 feet (9.14 m) and width of 250 feet (76.2 m). Finally, in 1968, it was dredged to its current dimensions.

2.2 Hurricane Laura

Hurricane Laura (2020) was a destructive, Category 4 hurricane that made landfall in this estuarine region near Cameron in southwest Louisiana in the early hours of August 27, 2020 (Jafari et al. 2020; Roueche et al. 2021; Fig. 2). It is tied with the Last Island Hurricane of 1856 as the strongest hurricane that made landfall in the state of Louisiana in terms of maximum sustained wind. It is also tied as the fifth strongest hurricane to make landfall in the continental USA and has set the record for the fastest intensification rate in the Gulf of Mexico (Roueche et al. 2021). Hurricane Laura formed from a large tropical wave that originated off the West African coast on August 16, 2020, then converted into a tropical depression on August 20, 2020, and finally made landfall on early August 27, 2020 (U.S. Census Bureau 2020; Roueche et al. 2021). Southwest Louisiana and southeast Texas were hit by winds up to 240 km/h and storm surge more than 3 m causing an estimated $19 billion in damages. Moreover, 33 people died in the state of Louisiana alone (NCEI 2021).

2.3 Data, model setup and model validation

Delft3D is an integrated modeling suite that can operate in different modes, such as 2D, Q3D or 3D (Elias et al. 2001). The 2D mode of Delft3D solves the depth-integrated, incompressible, Reynolds-averaged Navier–Stokes equations, or the nonlinear shallow-water equations (Symonds et al. 2017; Deltares 2020). It has been shown to be an effective tool to study coastal processes, including storm surge and hydrodynamic response to channel deepening (Hu et al. 2015; Zarzuelo et al. 2015; Wang et al. 2017; Hopkins et al. 2018; Liu et al. 2018; van Rijn and Grasmeijer 2018; van Rijn et al. 2018; Johnson et al. 2021; references therein and many others). We initialized Delft3D using the bathymetric data from USGS (Fig. 1). We forced the model using the observed wind and water-level data obtained from the NOAA station 8768094 at Calcasieu Pass, LA. The time series

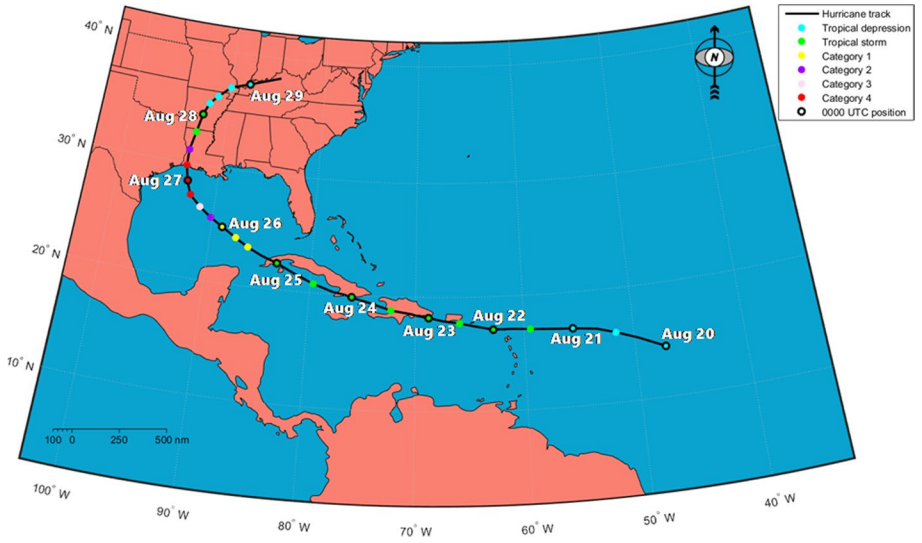

Fig. 2 Track of Hurricane Laura. The black solid line marks Hurricane Laura's track with different colored circles indicating the hurricane category over the course of ten days from August 20 to August 29 in the year 2020. Hurricane Laura made landfall in southwest Louisiana in the early hours of August 27, 2020

of the wind data (wind speed and wind direction) and the water-level data are shown in Fig. 3. We resolved the channel bathymetry using the NOAA nautical charts, combined with the coarser USGS map. These inputs were applied to a structured grid with uniform size of 20 m which spans 68.2 km in the horizontal and 54.66 km in the vertical direction (Fig. 1). We validated the model using observed water-level data from the USGS stations—08017118 in Calcasieu River at Cameron, LA and 08017095 in North Calcasieu Lake near Hackberry, LA (Fig. 1). From here on out, we will mention USGS 08017118 as USGS south and USGS 08017095 as USGS north for simplicity.

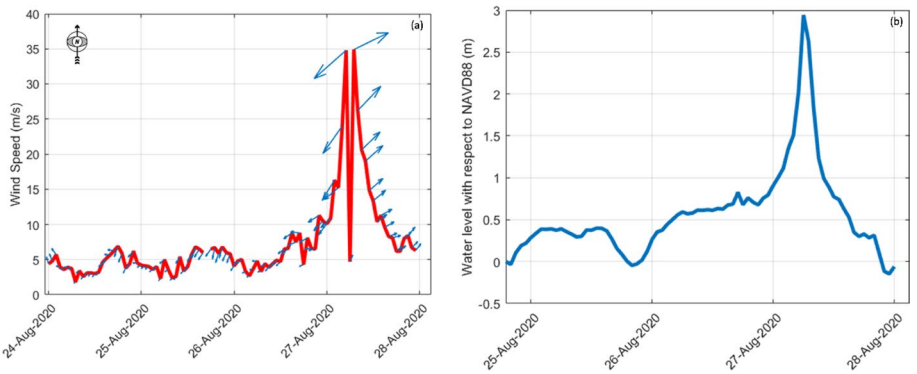

Fig. 3 **a** Date (*x*-axis) versus wind speed in meter per second (*y*-axis), with arrows representing wind direction (north being up) and the sizes of the arrows representing magnitude. **b** Date (*x*-axis) versus water level in meter relative to NAVD88 (*y*-axis). The data are obtained from the NOAA station 8768094 at Calcasieu Pass, LA

2.4 Channel depth scenarios

Four Calcasieu Ship Channel depth scenarios were simulated using Hurricane Laura wind forcing and observed water level to study how changing conditions affect the storm surge and the corresponding flooding situations. The channel depth scenarios are defined according to specific channel depth of specific years as follows:

- 40ft: 40 ft (12.19 m) as of the year 2020
- 30ft: 30 ft (9.14 m) as of the year 1941
- 13ft: 13 ft (3.96 m) as of the year 1903
- 5ft: 5 ft (1.52 m) as of first construction in the year 1874

2.5 Sea-level rise scenarios

We carried out numerical experiments for different sea-level rise (SLR) scenarios, in combination with the previously mentioned different channel depth scenarios, to study how changing sea-level conditions can affect the storm surge and the corresponding flooding situations. We selected three SLR scenarios based on the 2017 Coastal Master Plan of Louisiana to represent different possible future climate change conditions (Coastal Protection and Restoration Authority of Louisiana 2017). The three SLR scenarios are defined as follows:

- Low: a SLR value of 1.41 ft (0.43 m)
- Medium: a SLR value of 2.07 ft (0.63 m)
- High: a SLR value of 2.72 ft (0.83 m)

We did not consider the potential climate change effects on precipitation, evapotranspiration, subsidence, storm frequency and storm intensity for the purpose of this study, isolating the effects of sea-level rise.

One thing to be noted here is that the tests on the channel deepening are projections backward (2020–1874), while scenarios for SLR are projections forward. Some of these scenarios is never expected to happen. For example, the scenario combining the channel depth of 1874 and SLR will never happen for this specific site. Nonetheless, we run these combined scenarios to study how the same navigational channel with different historic water depths will respond differently to the same SLR implications. The goal is to examine how channel deepening over the years made the region more vulnerable to coastal flooding and how future SLR will make the already bad situation worse.

3 Results and discussion

We observe satisfactory model-data agreement (Fig. 4). The model skillfully simulates the fluctuations and the patterns of the observed water level at the two USGS station locations, although it is not perfect in capturing the minimum and the maximum. The maximum is under-predicted, and the minimum is over-predicted along with a slight temporal difference, north of Calcasieu Lake (Fig. 4b). Considering the order

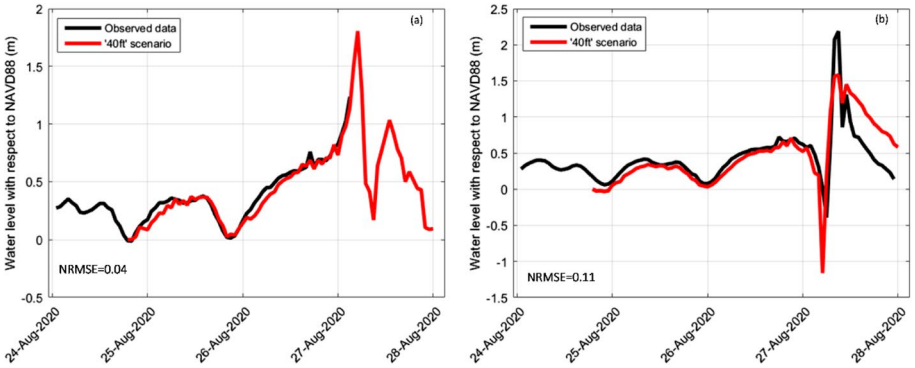

Fig. 4 Observed (black curves) and modeled (red curves) water level (relative to NAVD88) versus time at **a** USGS-south and **b** USGS-north stations' locations with 40 ft (12.19 m) deep ship channel. RMSE values (normalized by the observed data range) are given in the lower left corner. Notice that USGS-south station stopped working sometime after the hurricane landfall resulting in observation unavailability

of magnitude of the flood regime being studied (kilometers), these inaccuracies are expected to affect the flood vulnerability analysis only slightly.

Model results from different channel depth scenarios suggest that shallower channel blocks the water from going into the lake, whereas deeper channel facilitates water movement into the lake (Fig. 5). We believe that two processes drive this phenomenon—reduction in frictional resistance to water movement and increased channel cross-sectional area. In the momentum balance equation, the frictional term is inversely proportional to the depth (Jay 1991; Friedrichs and Aubrey 1994; Pullen et al. 2007; van Rijn 2011; Arns et al. 2017). At the same time, increase in channel depth increases the cross-sectional area of the channel which in turn increases the volume of water passing through the channel (Yorke 1978; Hughes 2002). As seen from the model results in Fig. 5a, the '5ft' (1.52 m) experiment produces a higher peak water level at the USGS-south station location in the ship channel. This peak gradually decreases for the other scenarios—lower for '13ft' (3.96 m) scenario and even lower for '30ft' (9.14 m) and '40ft' (12.19 m) cases (Fig. 5a). The USGS-north station shows the opposite—maximum peak water level for '40ft' scenario

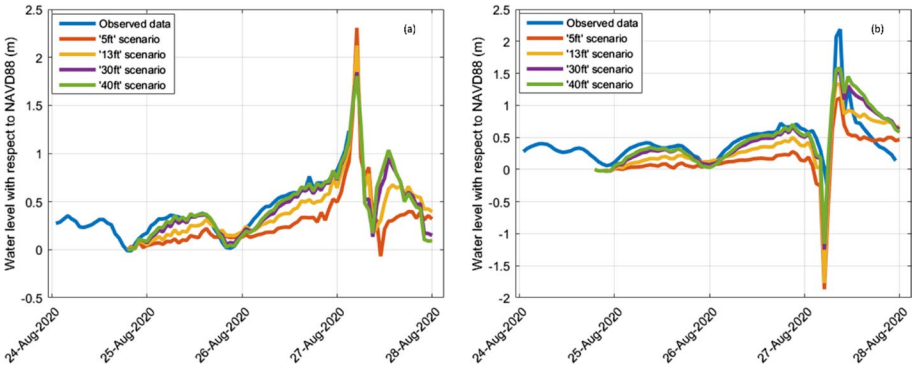

Fig. 5 Time series of water level (relative to NAVD88) for observations (blue), '5ft' (1.52 m, orange), '13ft' (3.96 m, yellow), '30ft' (9.14 m, violet) and '40ft' (12.19 m, green) scenarios at **a** USGS-south and **b** USGS-north stations' locations

and gradually decreasing with the minimum being that for '5ft' scenario (Fig. 5b). In comparison with the '5ft' scenario, the peak water level at this location has increased by 0.23 m (19%), 0.39 m (32.2%) and 0.45 m (37%) for '13ft,' '30ft' and '40ft' scenarios, respectively.

Peak water levels at different locations (and different times, given that the peak occurs earlier in the south than the north as the storm moves inland) in the study domain also suggest increased water movement through the ship channel with higher water depth during Hurricane Laura (Fig. 6). The figures infer that the higher peak water level for lower channel depth at the channel-lake mouth is caused due to 'piling-up' effect where the surge entering the channel from Gulf of Mexico is piling-up at the channel-lake mouth and not making it north. We observe substantial increase in the peak water level at different locations in and around Lake Calcasieu for '40ft' scenario as compared to the '5ft' one (Fig. 6d). This suggests that the channel depth can control storm surge movement into the lake.

Examining the momentum balance along the channel also suggests reduction in frictional resistance with increased channel depth and piling-up of water in the ship channel (Fig. 7). Generally, in the momentum balance equation for channels, pressure term ($g\ \partial\eta/\partial x$; g = acceleration due to gravity; η = water level) and friction term ($c_d\ u\ |u|/R$; c_d = drag coefficient; R = hydraulic radius $\approx h$ if $b >> h$; h = channel depth; b = channel width) are the most important. Local acceleration ($\partial u/\partial t$; u = cross-sectionally averaged velocity) and convective acceleration ($u\ \partial u/\partial x$) terms are relatively small (Friedrichs and Aubrey 1994; van Rijn 2011). Model results from different channel depth scenarios

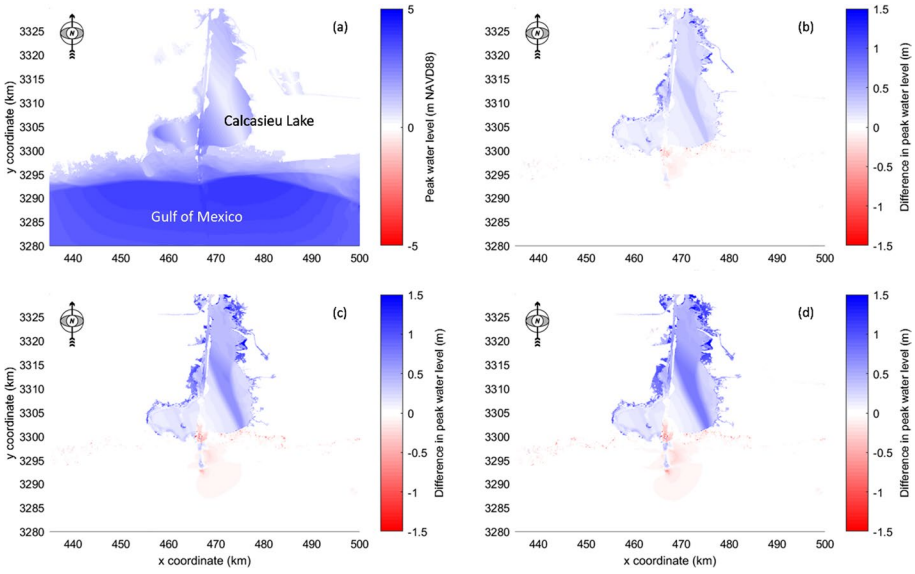

Fig. 6 **a** Peak water level relative to NAVD88 in meter at each grid point of the developed model in the presence of the '5ft' (1.52 m) channel after Hurricane Laura made landfall. The difference in the peak water level at each grid point between that of **b** '13ft' (3.96 m), **c** '30ft' (9.14 m) and **d** '40ft' (12.19 m) scenario, and the '5ft' scenario, with the red color meaning higher peak for the '5ft' scenario and blue meaning higher peak for the other scenarios. Notice that the water level reaches a higher peak in the channel-lake mouth for the '5ft' scenario, and at different locations in and around the lake for the other scenarios

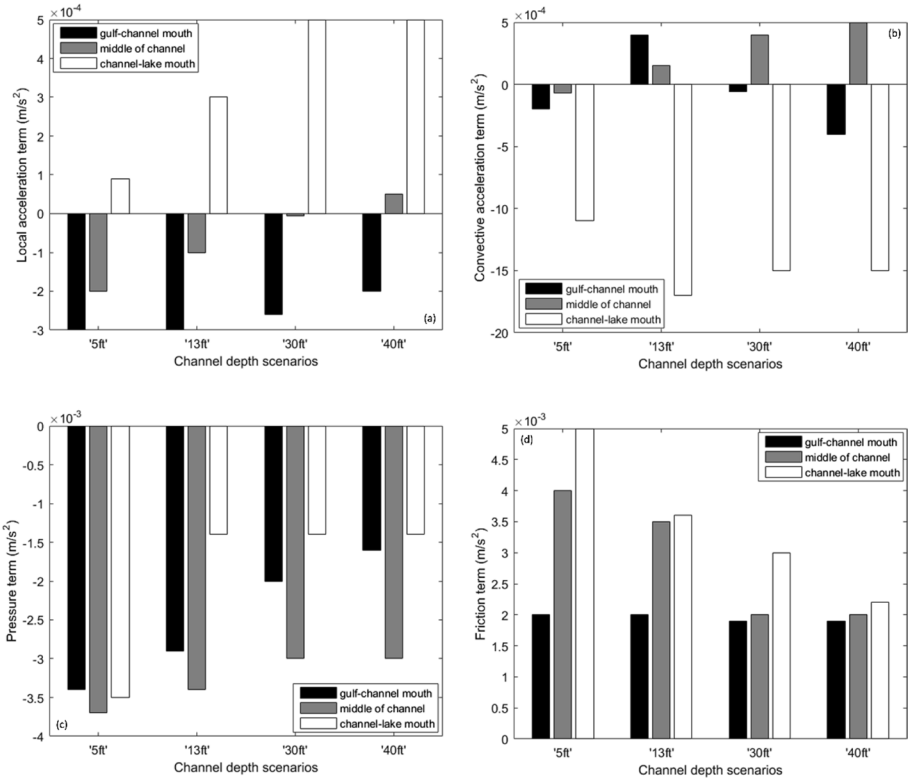

Fig. 7 Bar graph showing the terms in the momentum equation in the cross-shore direction along the Calcasieu Ship Channel at the time of peak water level at gulf-channel mouth for different channel depth scenarios: **a** local acceleration, **b** convective acceleration, **c** pressure or water surface slope and **d** bottom friction

also show that the local acceleration term and the convective acceleration term approximately differ by an order of magnitude from the pressure term and the friction term (Fig. 7). As seen from Fig. 7c, water surface slope between the gulf and the channel drives the momentum balance as the surge water flows through the channel. We observe higher water surface slope along the channel for the lower channel depth scenario as compared to the greater channel depth scenario. This suggests that for a shallower channel, the excess water gets piled-up more at the bay entrance and in the channel instead of flowing to the north. On the other hand, as seen from Fig. 7d, the friction term along the channel decreases with the increase in the channel depth, which facilitates water movement through the channel and into the lake. Thus, the channel depth controls the flow of the storm surge in the lake–estuary system.

Further, model results show that peak volumetric flow rates along Calcasieu Ship Channel increase with the increase in depth (Fig. 8). The '40ft' scenario produces the highest flow rate along the channel, whereas the '5ft' scenario produces the lowest (orange versus purple in Fig. 8). On average, as compared to '5ft' scenario, the percentage increase in peak flow rate along the channel is 73.7% for the '13ft' scenario, 215.8% for the '30ft' scenario and 291.6% for the '40ft' scenario.

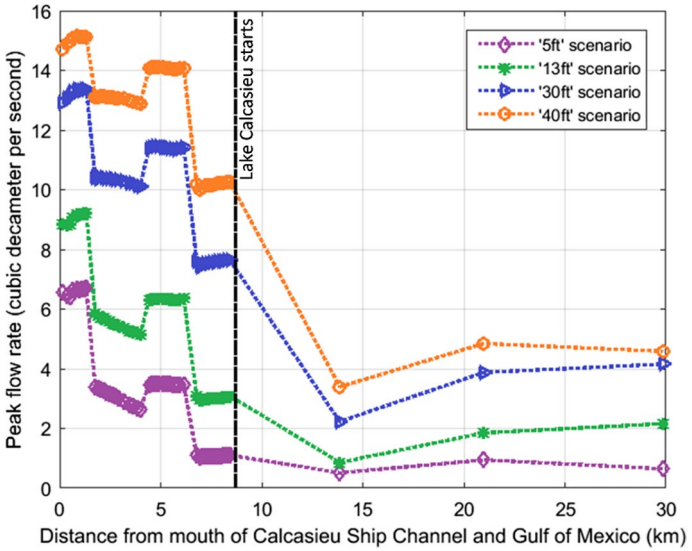

Fig. 8 Peak flow rate at various locations along the ship channel. The *x*-axis represents the distance in kilometers from mouth of Calcasieu Ship Channel and Gulf of Mexico, and the *y*-axis shows the peak flow rate. The plots are color-coded according to channel depth—purple for '5ft' (1.52 m), green for '13ft' (3.96 m), blue for '30ft' (9.14 m) and orange for '40ft' (12.19 m), respectively. The black dashed line marks the start of Calcasieu Lake

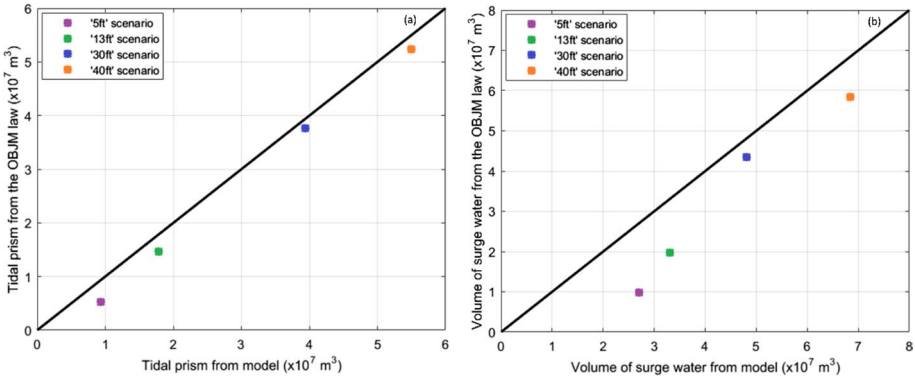

Fig. 9 **a** Tidal prism at Calcasieu Ship Channel inlet computed from simulation output (*x*-axis) versus empirical relationship (*y*-axis). **b** Volume of surge water passing through the same inlet cross section during Hurricane Laura computed from simulation output (*x*-axis) versus empirical relationship (*y*-axis). The plots are color-coded according to channel depth—purple for '5ft' (1.52 m), green for '13ft' (3.96 m), blue for '30ft' (9.14 m) and orange for '40ft' (12.19 m), respectively

Moreover, model results also show that tidal prism of the lake and the volume of surge water passing through the inlet increase with the increase in depth (Fig. 9). Tidal prism is the volume of water passing through an estuarine cross section or inlet on each tidal cycle (Lopes et al. 2013). Empirical relationships between tidal prism and channel or inlet cross-sectional area have been established in previous studies, and subsequent studies have confirmed their validity (O'Brien 1931, 1969; Jarrett 1976; Marchi 1990; D'Alpaos et al. 2010;

Hoitink et al. 2017; references therein and many others). The relationship, termed as the O'Brien–Jarrett–Marchi (OBJM) law (D'Alpaos et al. 2009, 2010), states that, $\Omega = k*P^{\alpha}$. Here, Ω is the channel or inlet cross-sectional area and P is the tidal prism with an exponent $\alpha = 6/7$ and $k = 1.2 \times 10^{-3}$ $m^{2-3\alpha}$, when Ω and P are expressed in m^2 and m^3, respectively (Marchi 1990; D'Alpaos et al. 2010). Tidal prism output from the Delft3D model of this study and the above empirical relationship are comparable, further validating the OBJM law for astronomical tides. However, in case of the storm tide, volume of surge water passing though the channel inlet, obtained from our model output, deviates slightly from the OBJM law. Nonetheless, it is found from the analysis that the '40ft' scenario produces the maximum tidal prism at the channel inlet, whereas the '5ft' scenario produces the minimum (orange versus purple in Fig. 9a). The trend is similar for the volume of surge water passing though the inlet: maximum for the '40ft' scenario and minimum for the '5ft' scenario (orange versus purple in Fig. 9b). Compared to the '5ft' scenario, the percentage increase in tidal prism is 90% for the '13ft' scenario, 320.5% for the '30ft' scenario and 487% for the '40ft' scenario. The corresponding percentage increase in the volume of surge water passing through the channel inlet is 22.6% for the '13ft' scenario, 78.1% for the '30ft' scenario and 153.3% for the '40ft' scenario.

Finally, simulations show an increase in flooded area for the '40ft' scenario as compared to other scenarios (Figs. 10, 11a). Compared to '5ft' experiment, each scenario exhibits notable increase in flooded area (blue, cyan and black areas in Fig. 10); the maximum is being observed for the '40ft' experiment. Area of new induced flooding for each of '13ft,' '30ft' and '40ft' scenario as compared to the '5ft' scenario is 24.9 km^2 (5.4% increase in the flooded area), 45.57 km^2 (9.8% increase) and 56.72 km^2 (12.2% increase), respectively. Some induced drying is also observed for each scenario near the coast and southern shore

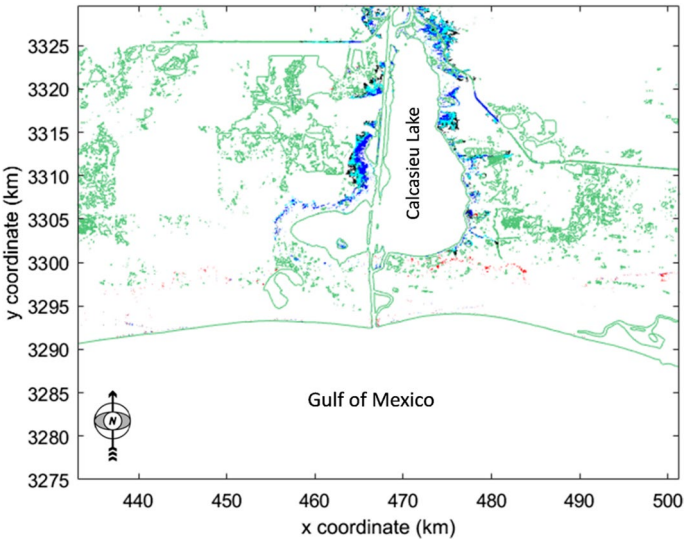

Fig. 10 New areas of induced flooding and drying for '13ft' (3.96 m), '30ft' (9.14 m) and '40ft' (12.19 m) scenario as compared to '5ft' (1.52 m) scenario. Blue color shows new areas of induced flooding for '13ft' scenario as compared to '5ft' scenario. Blue and cyan colors together are areas of new flooding for '30ft' scenario. Blue, cyan and black areas together are new flooding areas for '40ft' scenario. Red color shows new areas of induced drying for all three scenarios together when compared with '5ft' scenario. Green contour lines indicate the land edge

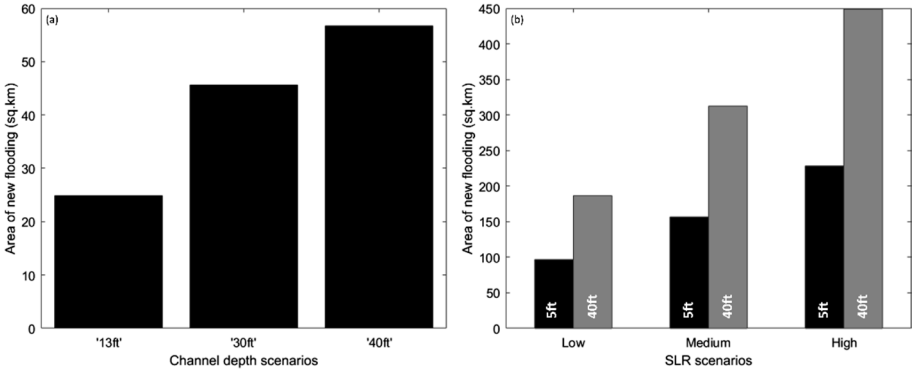

Fig. 11 **a** Bar graph showing the summary results of the area of new flooding in square kilometers for different channel depth scenarios (13 ft/3.96 m, 30 ft/9.14 m and 40 ft/12.19 m, respectively) as compared to the '5ft' (1.52 m) scenario and **b** bar graph showing the summary results of the area of new flooding in square kilometers for different SLR scenarios in the presence of the 5 ft (1.52 m) and 40 ft (12.19 m) deep channel when compared without SLR implications

of Lake Calcasieu (red areas in Fig. 10), likely because deeper channel conveys more water flow beyond the channel and into the lake, whereas shallower channel blocks the flow causing water to pile up inside the channel and leads to flooding of the overlying areas. However, areas of induced drying are negligible compared to those of induced flooding.

The wetlands in the surrounding area are expected to act as a vanguard against hurricane-induced flooding by preventing the storm surge from propagating inland. The potential of wetlands to mitigate hurricane-induced storm surge and the associated flooding is widely recognized (Loder et al. 2009; Wamsley et al. 2009; Barbier et al. 2013; Haddad et al. 2016; Zhao and Chen 2016; Narayan et al. 2017; references therein and many others). However, our results suggest that channel deepening can lead to increased storm surge penetration even in the presence of wetland vegetation, with the flooded area inland increasing drastically from changing the channel depth alone (Fig. 10).

Globally, channel deepening has been seen to produce alterations of tidal and storm surge amplitudes. Previous studies show instances of tidal amplification owing to channel deepening in various locations around the world including the Scheldt, Elbe, Ems and Loire River estuaries in Europe (Winterwerp et al. 2013), the Thames in the UK (Amin 1983), the Rhine-Meuse in Europe (Vellinga et al. 2014), the Weser estuary in Bremen, Germany (Winterwerp and Wang 2013), the Gironde estuary in France (Jalón-Rojas et al. 2018), the Cape Fear River Estuary in North Carolina, USA (Familkhalili and Talke 2016), the St. Johns River in Florida, USA (Bilskie 2013; Talke et al. 2021), the Chesapeake Bay estuary in the USA (Ross et al. 2017), the Pearl River estuary in China (Zhang et al. 2010, 2021), the Delaware River estuary on the East coast of the USA (DiLorenzo et al. 1993; Ross et al. 2017; Pareja-Roman et al. 2020), the Rotterdam waterway in the Netherlands (van Rijn et al. 2018), the Hudson River in the USA (Ralston et al. 2019), the Modaomen waterway in China (Cai et al. 2012b), the Columbia River in North America (Jay et al. 2011; Helaire et al. 2019), the Bay of Cádiz in Spain (Zarzuelo et al. 2015), Tampa Bay estuary in Florida, USA (Zhu et al. 2015), Newark Bay in New Jersey, USA (Chant et al. 2018), the Guadalquivir River estuary in Spain (Siles-Ajamil et al. 2019) and James River in Virginia, USA (Wang and Shen 2020). Storm surge, being shallow-water long waves like tides, undergoes amplification

as well, because of channel deepening. Previous studies show such instances of storm surge amplification in various locations in the USA including the Cape Fear River Estuary in North Carolina (Familkhalili and Talke 2016), Delaware Bay on the East Coast of the USA (Familkhalili et al. 2020) and Saint Johns River Estuary in Florida (Talke et al. 2021). Moreover, linkage between navigational channel deepening and flood risk has been investigated in some studies. Deepening of the Ria de Aveiro lagoon main channels in Portugal has been seen to induce an increase in the lagoon flood extent area (Lopes et al. 2013). In another study, it was suggested that coastal flooding in New York City can be mitigated by shallowing the channels around the city (Orton et al. 2015). A case study of the Pearl River Delta shows that channel deepening due to sand mining has increased peak water level in the tide-dominated coastal regions and the associated flood risk (Bao et al. 2022). An analytical model study also shows that deepening of an estuarine channel results in larger tidal amplitude and greater surge height causing large changes in the amplitude and spatial distribution of coastal flooding (Familkhalili et al. 2022). However, by contrast, channel deepening may reduce the flood level caused by river discharge, owing to increased hydraulic conveyance (Jensen et al. 2003; Jay et al. 2011; Helaire et al. 2019; Ralston et al. 2019). For example, in Albany, New York in the USA, located in the upper tidal river, although the tidal range has doubled and storm surge magnitude has increased over the past 150 years, the flood risk caused by large river discharge has significantly decreased (Ralston et al. 2019). Our findings are consistent with other studies that find that channel deepening facilitates inland storm surge propagation and increases the associated flood risk (Cai et al. 2012b; Lopes et al. 2013; Orton et al. 2015; references therein and many others).

The situation worsens under future SLR implications (Figs. 11b, 12). In the presence of the 5 ft (1.52 m) deep ship channel, the area of new flooding increases approximately 21%, 34% and 49% for the low, medium and high SLR scenarios respectively, when compared to no SLR (blue, cyan and black areas in Fig. 12a). With a 40ft (12.19 m) deep channel, we see even more flooding; again, for low, medium and high: approximately 36%, 60% and 86% increases, respectively (blue, cyan and black areas in

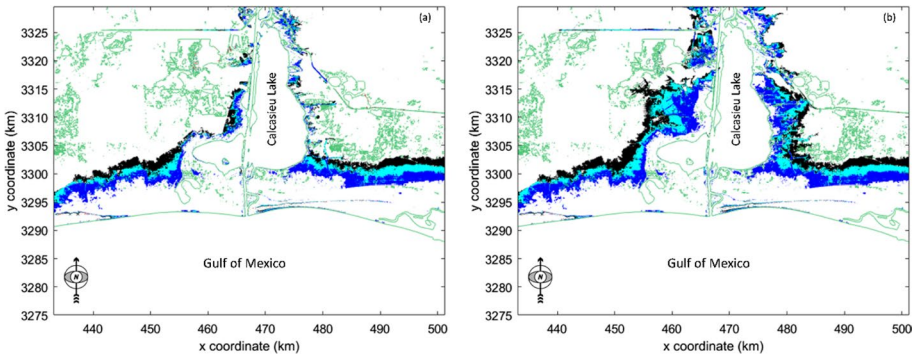

Fig. 12 New areas of induced flooding and drying for low, medium and high SLR scenario **a** in the presence of 5 ft (1.52 m) deep ship channel when compared with the previous '5ft' scenario and **b** in the presence of 40 ft (12.19 m) deep ship channel when compared with the previous '40ft' scenario. Blue color shows new areas of induced flooding for Low SLR scenario. Blue and cyan colors together are areas of new flooding for medium SLR scenario. Blue, cyan and black areas together are new flooding areas for high SLR scenario. Red color shows new areas of induced drying for all three scenarios. Green contour lines indicate the land edge

Fig. 12b). Even the most conservative scenario of SLR produced an approximately 51% increase in flooded area in the presence of the 40 ft deep ship channel, relative to the shallowest channel.

4 Conclusions

This study investigates the flood risk associated with channel deepening in an estuarine system during an extreme hurricane. Results from our numerical experiments suggest that channel deepening over the years has rendered the Calcasieu Lake estuarine region more vulnerable to hurricane-induced flooding. The presence of a deeper navigational channel facilitates water movement through the channel, resulting in increased surge penetration and increased flood risk. Flooded area increases almost 12% in case of the deepest channel scenario. Simulations also suggest that rising sea level is expected to make the already bad situation worse. According to our results, even the most conservative scenario of SLR will cause an approximately 51% increase in flooded area in the presence of the deepest ship channel. Considering the economic driver and other societal interests, it may be impractical not to administer dredging projects across the country. But proper research and cost–benefit analysis are imperative before implementing such projects, taking into consideration the damages resulting from increased flood events during extreme weather conditions, especially because of the current global climate change and rising sea levels. The Calcasieu Lake estuarine region may not be populated enough to cause as much damage as other densely populated coastal communities during such coastal flooding events. In a densely populated and highly urbanized coastal city, such as Boston or New York City, the damages can be ghastly. Numerous impervious parcels including unsewered paved roads and parking lots in urbanized areas will only add to the problem (Park et al. 2020; Blum et al. 2020; Feng et al. 2021). Therefore, the importance of additional state-of-the-art research into the matter cannot be overstated and needs to be continued.

Acknowledgements Funding for the study has been provided in part by the U.S. National Science Foundation (NSF Grants 2139882). Maqsood Mansur's work was partially supported by the Northeastern University Department of Civil and Environmental Engineering Fellowship. Any use of trade, firm, or product names is for descriptive purposes only and does not imply endorsement by the U.S. Government. We appreciate NOAA (National Oceanic and Atmospheric Administration), and USGS (United States Geological Survey) for providing the bathymetry data and the observed wind and water-level data.

Author contributions Maqsood Mansur contributed to methodology, formal analysis, data curation, writing—original draft preparation and visualization and provided software. Julia Hopkins was involved in conceptualization, methodology, validation, writing—review and editing, supervision and funding acquisition. Qin Chen contributed to conceptualization, methodology, validation, writing—review and editing, supervision and funding acquisition.

Funding Open access funding provided by Northeastern University Library. Funding for the study has been provided in part by the U.S. National Science Foundation (NSF Grants 2139882). Maqsood Mansur's work was partially supported by the Northeastern University Department of Civil and Environmental Engineering Fellowship.

Data availability Dataset containing the input data, model setup and simulation output is freely available in DesignSafe-CI (Rathje et al. 2017; Mansur et al. 2022).

Declarations

Competing interests The authors have no relevant financial or non-financial interests to disclose.

References

Amin M (1983) On perturbations of harmonic constants in the Thames Estuary. Geophys J Int 73:587–603. https://doi.org/10.1111/j.1365-246X.1983.tb03334.x

Arns A, Dangendorf S, Jensen J et al (2017) Sea-level rise induced amplification of coastal protection design heights. Sci Rep 7:1–9. https://doi.org/10.1038/srep40171

Bao S, Zhang W, Qin J et al (2022) Peak water level response to channel deepening depends on interaction between tides and the river flow. J Geophys Res Oceans. https://doi.org/10.1029/2021JC017625

Barbier EB, Georgiou IY, Enchelmeyer B, Reed DJ (2013) The value of wetlands in protecting southeast Louisiana from hurricane storm surges. PLoS ONE 8:e58715. https://doi.org/10.1371/journal.pone.0058715

Bilskie M (2013) Hydrodynamic modeling of tides and hurricane storm surge for pre-and post-dredging conditions in the lower St. Johns River, Florida. Ports 2013: Success through Diversification 1955–1964. https://doi.org/10.1061/9780784413067.200

Blum AG, Ferraro PJ, Archfield SA, Ryberg KR (2020) Causal effect of impervious cover on annual flood magnitude for the United States. Geophys Res Lett. https://doi.org/10.1029/2019GL086480

Burchard H, Schuttelaars HM, Ralston DK (2018) Sediment trapping in estuaries. Ann Rev Mar Sci 10:371–395. https://doi.org/10.1146/annurev-marine-010816-060535

Cai H, Savenije HHG, Toffolon M (2012a) A new analytical framework for assessing the effect of sea-level rise and dredging on tidal damping in estuaries. J Geophys Res Oceans. https://doi.org/10.1029/2012aJC008000

Cai H, Savenije HHG, Yang Q et al (2012b) Influence of river discharge and dredging on tidal wave propagation: Modaomen Estuary case. J Hydraul Eng 138:885–896. https://doi.org/10.1061/(ASCE)HY.1943-7900.0000594

Calcasieu Ship Channel (2021) Port of Lake Charles. https://portlc.com/calcasieu-ship-channel/. Accessed 14 Dec 2021

Chant RJ, Sommerfield CK, Talke SA (2018) Impact of channel deepening on tidal and gravitational circulation in a highly engineered estuarine basin. Estuaries Coasts 41:1587–1600. https://doi.org/10.1007/s12237-018-0379-6

Chen W-B, Liu W-C (2016) Assessment of storm surge inundation and potential hazard maps for the southern coast of Taiwan. Nat Hazards 82:591–616. https://doi.org/10.1007/s11069-016-2199-y

Coastal Protection and Restoration Authority of Louisiana (2017) Louisiana's Comprehensive Master Plan for a Sustainable Coast. Baton Rouge, LA

Cox R, Wadsworth RA, Thomson AG (2003) Long-term changes in salt marsh extent affected by channel deepening in a modified estuary. Cont Shelf Res 23:1833–1846. https://doi.org/10.1016/j.csr.2003.08.002

CWPPRA (1992) Calcasieu-Sabine River Basin Study. New Orleans, LA

D'Alpaos A, Lanzoni S, Marani M, Rinaldo A (2009) On the O'Brien–Jarrett–Marchi law. RENDICONTI LINCEI 20:225–236. https://doi.org/10.1007/s12210-009-0052-x

D'Alpaos A, Lanzoni S, Marani M, Rinaldo A (2010) On the tidal prism–channel area relations. J Geophys Res Earth Surf. https://doi.org/10.1029/2008JF001243

de Jonge VN, Schuttelaars HM, van Beusekom JEE et al (2014) The influence of channel deepening on estuarine turbidity levels and dynamics, as exemplified by the Ems estuary. Estuar Coast Shelf Sci 139:46–59. https://doi.org/10.1016/j.ecss.2013.12.030

Deltares (2020) Delft3d-flow, simulation of multi-dimensional hydrodynamic flows and transport phenomena, including sediments. User Manual, Version: 315, May 2020

Dijkstra YM, Schuttelaars HM, Schramkowski GP, Brouwer RL (2019) Modeling the transition to high sediment concentrations as a response to channel deepening in the Ems River Estuary. J Geophys Res Oceans 124:1578–1594. https://doi.org/10.1029/2018JC014367

DiLorenzo JL, Huang P, Thatcher ML, Najarian TO (1993) Dredging impacts on Delaware Estuary tides. In: Estuarine and coastal modeling. ASCE, pp 86–104

Elias EPL, Walstra DJR, Roelvink JA et al (2001) Hydrodynamic validation of Delft3D with field measurements at Egmond. Coast Eng 2000:2714–2727. https://doi.org/10.1061/40549(276)212

Emanuel K (2005) Increasing destructiveness of tropical cyclones over the past 30 years. Nature 436:686–688. https://doi.org/10.1038/nature03906

Emanuel K (2020) Evidence that hurricanes are getting stronger. Proc Natl Acad Sci 117:13194–13195. https://doi.org/10.1073/pnas.2007742117

Emanuel K (2021) Atlantic tropical cyclones downscaled from climate reanalyses show increasing activity over past 150 years. Nat Commun 12:7027. https://doi.org/10.1038/s41467-021-27364-8

Familkhalili R, Talke SA (2016) The effect of channel deepening on tides and storm surge: a case study of Wilmington, NC. Geophys Res Lett 43:9138–9147. https://doi.org/10.1002/2016GL069494

Familkhalili R, Talke SA, Jay DA (2020) Tide-storm surge interactions in highly altered estuaries: how channel deepening increases surge vulnerability. J Geophys Res Oceans. https://doi.org/10.1029/2019JC015286

Familkhalili R, Talke SA, Jay DA (2022) Compound flooding in convergent estuaries: insights from an analytical model. Ocean Sci 18:1203–1220. https://doi.org/10.5194/os-18-1203-2022

Feng B, Zhang Y, Bourke R (2021) Urbanization impacts on flood risks based on urban growth data and coupled flood models. Nat Hazards 106:613–627. https://doi.org/10.1007/s11069-020-04480-0

Friedrichs CT, Aubrey DG (1994) Tidal propagation in strongly convergent channels. J Geophys Res Oceans 99:3321–3336. https://doi.org/10.1029/93JC03219

Gero A, Méheux K, Dominey-Howes D (2011) Integrating disaster risk reduction and climate change adaptation in the Pacific. Clim Dev 3:310–327. https://doi.org/10.1080/17565529.2011.624791

Haddad J, Lawler S, Ferreira CM (2016) Assessing the relevance of wetlands for storm surge protection: a coupled hydrodynamic and geospatial framework. Nat Hazards 80:839–861. https://doi.org/10.1007/s11069-015-2000-7

Helaire LT, Talke SA, Jay DA, Mahedy D (2019) Historical changes in lower Columbia River and Estuary floods: a numerical study. J Geophys Res Oceans 124:7926–7946. https://doi.org/10.1029/2019JC015055

Hoitink AJF, Wang ZB, Vermeulen B et al (2017) Tidal controls on river delta morphology. Nat Geosci 10:637–645. https://doi.org/10.1038/ngeo3000

Holland GJ, Webster PJ (2007) Heightened tropical cyclone activity in the North Atlantic: natural variability or climate trend? Philos Trans R Soc A Math Phys Eng Sci 365:2695–2716. https://doi.org/10.1098/rsta.2007.2083

Hopkins J, Elgar S, Raubenheimer B (2018) Storm impact on morphological evolution of a sandy inlet. J Geophys Res Oceans 123:5751–5762. https://doi.org/10.1029/2017JC013708

Hu K, Chen Q, Wang H (2015) A numerical study of vegetation impact on reducing storm surge by wetlands in a semi-enclosed estuary. Coast Eng 95:66–76. https://doi.org/10.1016/j.coastaleng.2014.09.008

Hughes SA (2002) Equilibrium cross sectional area at tidal inlets. J Coast Res 160–174

Islam S, Chu C, Smart JCR (2020) Challenges in integrating disaster risk reduction and climate change adaptation: exploring the Bangladesh case. Int J Disaster Risk Reduct 47:101540. https://doi.org/10.1016/j.ijdrr.2020.101540

Jafari NH, Chen Q, Cadigan J (2020) Rapid deployment and post-storm reconnaissance of Hurricane Laura. Coastal Eng Proc. https://doi.org/10.9753/icce.v36v.waves.60

Jalón-Rojas I, Sottolichio A, Hanquiez V et al (2018) To what extent multidecadal changes in morphology and fluvial discharge impact tide in a convergent (turbid) tidal river. J Geophys Res Oceans 123:3241–3258. https://doi.org/10.1002/2017JC013466

Jarrett JT (1976) Tidal prism-inlet area relationships. US Army Engineer Waterways Experiment Station

Jay DA (1991) Green's law revisited: tidal long-wave propagation in channels with strong topography. J Geophys Res Oceans 96:20585–20598. https://doi.org/10.1029/91JC01633

Jay DA, Leffler K, Degens S (2011) Long-term evolution of Columbia River tides. J Waterw Port Coast Ocean Eng 137:182–191. https://doi.org/10.1061/(ASCE)WW.1943-5460.0000082
Jensen J, Mudersbach C, Blasi C (2003) Hydrological changes in tidal estuaries due to natural and anthropogenic effects. In: 6th international MEDCOAST 2003 conference, Ravenna, Italy
Johnson CL, Chen Q, Ozdemir CE et al (2021) Morphodynamic modeling of a low-lying barrier subject to hurricane forcing: the role of backbarrier wetlands. Coast Eng 167:103886. https://doi.org/10.1016/j.coastaleng.2021.103886
Karim MF, Mimura N (2008) Impacts of climate change and sea-level rise on cyclonic storm surge floods in Bangladesh. Glob Environ Chang 18:490–500. https://doi.org/10.1016/j.gloenvcha.2008.05.002
Kaur J, Jaligama G, Atkinson JF et al (2007) Modeling dissolved oxygen in a Dredged Lake Erie Tributary. J Great Lakes Res 33:62–82. https://doi.org/10.3394/0380-1330(2007)33[62:MDOIAD]2.0.CO;2
Kerner M (2007) Effects of deepening the Elbe Estuary on sediment regime and water quality. Estuar Coast Shelf Sci 75:492–500. https://doi.org/10.1016/j.ecss.2007.05.033
Kim KW, Johnson BH (1998) Assessment of channel deepening in the Delaware River and Bay. A three-dimensional numerical model study. Army Engineer Waterways Experiment Station Vicksburg MS
Klotzbach PJ, Wood KM, Schreck CJ III et al (2022) Trends in global tropical cyclone activity: 1990–2021. Geophys Res Lett. https://doi.org/10.1029/2021GL095774
Knutson TR, McBride JL, Chan J et al (2010) Tropical cyclones and climate change. Nat Geosci 3:157–163. https://doi.org/10.1038/ngeo779
Lee JM, Wiseman WJ, Kelly FJ (1990) Barotropic, subtidal exchange between Calcasieu Lake and the Gulf of Mexico. Estuaries 13:258–264. https://doi.org/10.2307/1351916
Liu K, Chen Q, Hu K et al (2018) Modeling hurricane-induced wetland-bay and bay-shelf sediment fluxes. Coast Eng 135:77–90. https://doi.org/10.1016/j.coastaleng.2017.12.014
Loder NM, Irish JL, Cialone MA, Wamsley TV (2009) Sensitivity of hurricane surge to morphological parameters of coastal wetlands. Estuar Coast Shelf Sci 84:625–636. https://doi.org/10.1016/j.ecss.2009.07.036
Lopes CL, Plecha S, Silva PA, Dias JM (2013) Influence of morphological changes in a lagoon flooding extension: case study of Ria de Aveiro (Portugal). J Coast Res 2013:1158–1163. https://doi.org/10.2112/SI65-196.1
Manning J (2021) Gen. Honore to urge officials not to build gas terminals in hurricane-prone areas. KPLC 7 News
Mansur M, Hopkins J, Chen Q (2022) "Delft3D model runs", in Data, model setup and simulation output from “Estuarine response to storm surge and sea level rise associated with channel deepening: A flood vulnerability assessment of southwest Louisiana, USA.” DesignSafe-CI. https://doi.org/10.17603/ds2-2acf-2y97
Marchi E (1990) Sulla stabilità delle bocche lagunari a marea. Rendiconti Lincei 1:137–150. https://doi.org/10.1007/BF03001888
Martin Associates (2021) THE ECONOMIC IMPACTS OF THE CALCASIEU SHIP CHANNEL. https://portlc.com/wp-content/uploads/2021/12/PORT.Executive-Summary-2021-POLC-Economic-Impact-Study.pdf. Accessed 29 Mar 2022
McGinnis TE, Wood WB, Luent M et al (2019) 2019 basin summary report for the Calcasieu-Sabine Basin. Coastal Protection and Restoration Authority of Louisiana, Lafayette, Louisiana 59
Mitchell T, van Aalstm M, Silva Villanueva P (2010) Assessing progress on integrating disaster risk reduction and climate change adaptation in development processes. In: Strengthening Climate Resilience Discussion. Institute of Development Studies. University of Sussex
Narayan S, Beck MW, Wilson P et al (2017) The value of coastal wetlands for flood damage reduction in the Northeastern USA. Sci Rep 7:9463. https://doi.org/10.1038/s41598-017-09269-z
NOAA National Centers for Environmental Information (NCEI) (2021) U.S. Billion-Dollar Weather and Climate Disasters. https://www.ncdc.noaa.gov/billions/. Accessed 22 Feb 2022
O’Brien MP (1931) Estuary tidal prisms related to entrance areas. Civ Eng 1:738–739
O’Brien MP (1969) Equilibrium flow areas of inlets on sandy coasts. J Waterways Harbors Div 95:43–52. https://doi.org/10.1061/JWHEAU.0000622
Orton PM, Talke SA, Jay DA et al (2015) Channel shallowing as mitigation of coastal flooding. J Mar Sci Eng 3:654–673. https://doi.org/10.3390/jmse3030654
Orton PM, Conticello FR, Cioffi F et al (2020) Flood hazard assessment from storm tides, rain and sea level rise for a tidal river estuary. Nat Hazards 102:729–757. https://doi.org/10.1007/s11069-018-3251-x
Pareja-Roman LF, Chant RJ, Sommerfield CK (2020) Impact of historical channel deepening on tidal hydraulics in the Delaware Estuary. J Geophys Res Oceans. https://doi.org/10.1029/2020JC016256

Park H, Paterson R, Zigmund S et al (2020) The effect of coastal city development on flood damage in South Korea. Sustainability 12:1854. https://doi.org/10.3390/su12051854
Pullen T, Allsop NWH, Bruce T, et al (2007) EurOtop wave overtopping of sea defences and related structures: assessment manual
Rahman A, Yunus A (2016) Hydrodynamic and morphological response to dredging: analysis on Gorai river of Bangladesh. Int J Innov Res Sci Eng Technol 5:15610–15618
Ralston DK, Geyer WR (2019) Response to channel deepening of the salinity intrusion, estuarine circulation, and stratification in an urbanized estuary. J Geophys Res Oceans 124:4784–4802. https://doi.org/10.1029/2019JC015006
Ralston DK, Talke S, Geyer WR et al (2019) Bigger tides, less flooding: effects of dredging on barotropic dynamics in a highly modified estuary. J Geophys Res Oceans 124:196–211. https://doi.org/10.1029/2018JC014313
Rathje EM, Dawson C, Padgett JE et al (2017) DesignSafe: new cyberinfrastructure for natural hazards engineering. Nat Hazards Rev 18:06017001. https://doi.org/10.1061/(ASCE)NH.1527-6996.0000246
Rego JL, Li C, Hossain I (2010) The Flushing of Louisiana's coastal bays under hurricane conditions. Estuar Coast Model 2009:89–107. https://doi.org/10.1061/41121(388)6
Ross AC, Najjar RG, Li M et al (2017) Fingerprints of sea level rise on changing tides in the Chesapeake and Delaware Bays. J Geophys Res Oceans 122:8102–8125. https://doi.org/10.1002/2017JC012887
Roueche D, Kameshwar S, Marshall J, et al (2021) Hybrid Preliminary Virtual Reconnaissance Report-Early Access Reconnaissance Report (PVRR-EARR)
Sangita S, Satapathy DR, Kar RN, Panda CR (2014) Impact of dredging on coastal water quality of dhamra, Orissa. Indian J Geo-Mar Sci 43:33–38
Serrao-Neumann S, Crick F, Harman B et al (2015) Maximising synergies between disaster risk reduction and climate change adaptation: Potential enablers for improved planning outcomes. Environ Sci Policy 50:46–61. https://doi.org/10.1016/j.envsci.2015.01.017
Shepard CC, Agostini VN, Gilmer B et al (2012) Assessing future risk: quantifying the effects of sea level rise on storm surge risk for the southern shores of Long Island, New York. Nat Hazards 60:727–745. https://doi.org/10.1007/s11069-011-0046-8
Siles-Ajamil R, Díez-Minguito M, Losada MÁ (2019) Tide propagation and salinity distribution response to changes in water depth and channel network in the Guadalquivir River Estuary: An exploratory model approach. Ocean Coast Manag 174:92–107. https://doi.org/10.1016/j.ocecoaman.2019.03.015
Symonds AM, Vijverberg T, Post S et al (2017) Comparison between mike 21 FM, DELFT3D and DELFT3D FM flow models of western port bay, Australia. Coast Eng Proc 11:10. https://doi.org/10.9753/icce.v35.currents.11
Talke SA, Familkhalili R, Jay DA (2021) The influence of channel deepening on tides, river discharge effects, and storm surge. J Geophys Res Oceans. https://doi.org/10.1029/2020JC016328
Tasnim KM, Shibayama T, Esteban M et al (2015) Field observation and numerical simulation of past and future storm surges in the Bay of Bengal: case study of cyclone Nargis. Nat Hazards 75:1619–1647. https://doi.org/10.1007/s11069-014-1387-x
U.S. Census Bureau (2020) 2020 Hurricane Laura. https://www.census.gov/topics/preparedness/events/hurricanes/laura.html. Accessed 6 Apr 2022
van Rijn LC (2011) Analytical and numerical analysis of tides and salinities in estuaries; part I: tidal wave propagation in convergent estuaries. Ocean Dyn 61:1719–1741. https://doi.org/10.1007/s10236-011-0453-0
van Rijn L, Grasmeijer B (2018) Effect of channel deepening on tidal flow and sediment transport—part II: muddy channels. Ocean Dyn 68:1481–1501. https://doi.org/10.1007/s10236-018-1205-1
van Maren DS, van Kessel T, Cronin K, Sittoni L (2015) The impact of channel deepening and dredging on estuarine sediment concentration. Cont Shelf Res 95:1–14. https://doi.org/10.1016/j.csr.2014.12.010
van Rijn L, Grasmeijer B, Perk L (2018) Effect of channel deepening on tidal flow and sediment transport: part I—sandy channels. Ocean Dyn 68:1457–1479. https://doi.org/10.1007/s10236-018-1204-2
Vecchi GA, Landsea C, Zhang W et al (2021) Changes in Atlantic major hurricane frequency since the late-19th century. Nat Commun 12:4054. https://doi.org/10.1038/s41467-021-24268-5
Vellinga NE, Hoitink AJF, van der Vegt M et al (2014) Human impacts on tides overwhelm the effect of sea level rise on extreme water levels in the Rhine-Meuse delta. Coast Eng 90:40–50. https://doi.org/10.1016/j.coastaleng.2014.04.005
Wamsley TV, Cialone MA, Smith JM et al (2009) Influence of landscape restoration and degradation on storm surge and waves in southern Louisiana. Nat Hazards 51:207–224. https://doi.org/10.1007/s11069-009-9378-z

Wang Y, Shen J (2020) A modeling study on the influence of sea-level rise and channel deepening on estuarine circulation and dissolved oxygen levels in the tidal James River, Virginia, USA. J Mar Sci Eng 8:950. https://doi.org/10.3390/jmse8110950

Wang H, Chen Q, Hu K et al (2017) Numerical modeling of the effects of Hurricane Sandy and potential future hurricanes on spatial patterns of salt marsh morphology in Jamaica Bay, New York City. US Geol Surv Open-File Rep 2017–1016:43. https://doi.org/10.3133/ofr20171016

Wang J, Li C, Xu F, Huang W (2020) Severe weather-induced exchange flows through a narrow tidal channel of Calcasieu Lake Estuary. J Mar Sci Eng. https://doi.org/10.3390/jmse8020113

Winterwerp JC, Wang ZB (2013) Man-induced regime shifts in small estuaries—I: theory. Ocean Dyn 63:1279–1292. https://doi.org/10.1007/s10236-013-0662-9

Winterwerp JC, Wang ZB, van Braeckel A et al (2013) Man-induced regime shifts in small estuaries—II: a comparison of rivers. Ocean Dyn 63:1293–1306. https://doi.org/10.1007/s10236-013-0663-8

Yorke TH (1978) Impact assessment of water resource development activities: a dual matrix approach. Department of the Interior, Fish and Wildlife Service, Eastern Energy and Land Use Team

Zarzuelo C, Díez-Minguito M, Ortega-Sánchez M et al (2015) Hydrodynamics response to planned human interventions in a highly altered embayment: the example of the Bay of Cádiz (Spain). Estuar Coast Shelf Sci 167:75–85. https://doi.org/10.1016/j.ecss.2015.07.010

Zhang W, Ruan X, Zheng J et al (2010) Long-term change in tidal dynamics and its cause in the Pearl River Delta, China. Geomorphology 120:209–223. https://doi.org/10.1016/j.geomorph.2010.03.031

Zhang P, Yang Q, Wang H et al (2021) Stepwise alterations in tidal hydrodynamics in a highly human-modified estuary: the roles of channel deepening and narrowing. J Hydrol (amst) 597:126153. https://doi.org/10.1016/j.jhydrol.2021.126153

Zhao H, Chen Q (2016) Modeling attenuation of storm surge over deformable vegetation: parametric study. J Eng Mech 142:06016006. https://doi.org/10.1061/(ASCE)EM.1943-7889.0001109

Zhu J, Weisberg RH, Zheng L, Han S (2015) Influences of channel deepening and widening on the tidal and nontidal circulations of Tampa Bay. Estuar Coasts 38:132–150. https://doi.org/10.1007/s12237-014-9815-4